Modeling the Spontaneous Ignition of Coal Stockpiles

Andrew G. Salinger, Rutherford Aris, and Jeffrey J. Derby
Dept. of Chemical Engineering and Materials Science, University of Minnesota, Minneapolis, MN 55455

The spontaneous ignition of coal stockpiles is a serious economic and safety problem. This phenomenon is analyzed using the approach of modern reaction engineering, which is made challenging by the nonlinear interactions of chemical reaction, heat transfer, and buoyancy-driven flows within and around the stockpile. A model developed represents reaction and transport within a realistically-shaped stockpile and transport and flow in the surrounding air. A new methodology based on the Galerkin finite-element method (Salinger, 1993b) allows for efficient solution of flows in both porous and open domains. Bifurcation analysis is used to track steady-state model solutions of relevant parameters, such as the Damköhler number (dimensionless reaction rate), Rayleigh number (dimensionless driving force for buoyant flow), and dimensionless permeability of the stockpile. The solutions provide an understanding of the roles of various transport mechanisms on the ignition behavior and nonlinear coupling between these mechanisms. Results clearly demonstrate the need for incorporating realistic descriptions of flow and transport in the surrounding air into the model.

Introduction

Chemical reactors have often provided the setting for the mathematical analysis of coupled reaction and transport (Aris, 1975; Aris and Varma, 1980; Hlavacek, 1986). Much prior work has concentrated on lumped parameter systems, such as the continuous-flow stirred-tank reactor, where assumptions such as perfect mixing make the consideration of transport effects trivial (Uppal et al., 1974; Balakotaiah and Luss, 1983, 1984). A more realistic accounting for transport is allowed in distributed parameter systems, such as the plug-flow tubular reactor (Jensen and Ray, 1982), but even here effects such as fluid flow are usually greatly simplified. More recently, reaction engineering studies have addressed the rigorous modeling of coupled flow and reaction (for example, Jensen, 1987; Song et al., 1991). In this study, we consider coupled chemical reaction, mass transport, and natural convective flows during the spontaneous ignition of a coal stockpile.

Coal reacts exothermally with the oxygen in the air while being shipped to and stored at utility plants. Under certain conditions, the heat generated from this reaction can cause the pile to ignite spontaneously (Williamson, 1982). This study investigates the behavior of coal piles over a wide range of conditions to understand the physical phenomena that influence spontaneous ignition. Of particular interest are buoyancy-driven flows driven by thermal gradients in the system and the nonlinear coupling of these flows with transport and reaction. The effect of natural convection on ignition is difficult to predict *a priori*, for the reaction is fueled by the increase in oxygen transport but damped by the accompanying convective cooling.

Coal stockpile ignition is an interesting example of a reacting system which involves flows driven by natural convection coupled with chemical reaction in porous media. There is a large body of literature dealing with buoyant flow through porous media. Lapwood (1948) predicted the onset of convection in a porous medium bounded by two isothermal planes at different temperatures. Numerous other researchers have studied finite-amplitude convective flows in porous media arising from imposed temperature boundary conditions which result in driving density gradients (Strauss, 1974; Caltagirone, 1975). Flows driven by buoyant effects arising from the volumetric heat generation of chemical reaction were studied by Viljoen and Hlavacek (1987), Gatica et al. (1989), and Farr et al. (1991).

Much study has also been devoted to describing chemical

Correspondence concerning this article should be addressed to J. J. Derby.

Table 1. Taxonomy of Prior Coal Stockpile Ignition Models and Assumptions

Models	van Doornum (1954)	Nordon (1979)	Schmal et al. (1985)	Young et al. (1986)	Brooks & Glasser (1986)	Brooks et al. (1988b,c)	Brooks et al. (1988a)	Bradshaw et al. (1991)	This Work
Spatial Dimensionality	0	1	1	2	1	1	2	3	2
Transient (*T*) or Steady State (*SS*)	*T*	*T*	*T*	*SS*	*SS*	*SS*	*SS*	*SS*	*SS*
Exponential Heat Generation	*X*	*X*	*X*		*X*	*X*	*X*	*X*	*X*
Oxygen Concentration		*X*	*X*		*X*	*X*	*X*		*X*
Convection, Forced (*F*) or Natural (*N*)		*F*	*F*	*N*	*N*	*N*	*N*	*N*	*N*
Compressibility of Fluid Phase					*X*	*X*	*X*		*X*
Bifurcation Analysis						*X*		*X*	*X*
Surrounding Air									*X*

reactor systems where instabilities give rise to runaway behavior, such as the study of ignition phenomena in combustion systems. The approach of Frank-Kamenetskii and coworkers (Zeldovich and Frank-Kamenetskii, 1938; Frank-Kamenetskii, 1969), which decoupled flow behavior from heat and mass balances, has been widely adopted. Relatively little research exists on the effects of natural convection on these processes. Merzhanov and Shtessel (1973), Jones (1974), and Shtessel et al. (1978) studied ignition in homogeneous systems as a function of the Frank-Kamenetskii parameter, which is the ratio of rates of heat generated by reaction to that dissipated by conduction. They concluded that natural convection can increase by several times the critical value of the Frank-Kamenetskii parameter over the value calculated when conduction is the only heat-transport mechanism, thereby delaying the onset of thermal ignition. Kordylewski and Krajewski (1984), in their study on the effects of convection on thermal ignition in porous media, concluded that convection causes critical conditions of thermal ignition to shift to higher temperatures than those calculated allowing for conduction alone. These studies indicated that natural convection has a stabilizing influence on potentially explosive systems. Viljoen et al. (1988) studied the effect of convection on ignition transients in porous media. They showed that, in addition to the magnitude of convection, the induction time needed for flow development determined critical ignition conditions. Balakotaiah and Pourtalet (1990a,b) extensively studied a one-dimensional model for diffusion, convection, and reaction in a porous medium and developed explicit relationships for criticality as a function of Rayleigh number.

The spontaneous ignition of a coal stockpile combines many aspects of the studies described above; Table 1 classifies prior models for this system. Van Doornum (1954) solved a time-dependent equation for a lumped coal pile temperature to predict storage situations where precautions should be taken against ignition. In this model, the heat generation rate is assumed to increase exponentially with temperature and decay exponentially in time, while a linear heat loss term models dissipation. The model neglects any effects of oxygen depletion or convection. Nordon (1979) includes these two effects in a packed-bed model of self-heating char. Dankwerts' boundary conditions are used to model the oxygen concentration, water vapor concentration, and temperature along the length of the bed. The temporal evolution of the temperature profile is calculated for various values of the imposed flow rate. Reaction kinetic data were measured experimentally in related articles (Nordon et al., 1979; Nordon and Bainbridge, 1979). Schmal et al. (1985) employed a similar model to study the effects of air flow rate, coal porosity, reaction rate, and initial temperature on stockpile ignition. Both of these models (Nordon, 1979; Schmal et al., 1985) analyzed forced convection through the packed bed by arbitrarily varying the air flow velocity as a system parameter.

More recent models attempted to solve for natural convective flows in the porous coal stockpile. Young et al. (1986) considered convection driven by a point source of heat in a 2-D cavity which was open at the top and closed on the sides and bottom. Both natural convection and reactant concentration effects were included in the 1-D model of Brooks and Glasser (1986). This work modeled the coal pile as a "chimney," a vertical packed bed with a plug-flow velocity field, and temperature, oxygen concentration, and pressure were considered as functions of distance up the bed. The scalar air speed was calculated from the overall pressure drop, which in turn depended on the temperature and flow rate. The authors found that coal piles were safe when the coal particles were either small or large. In the former case, the system was oxygen-limited and only the surface of the particle reacted, while in the latter, strong cooling homogenized the temperature field before a hot spot could develop. Brooks et al. (1988b) studied the multiplicity behavior of the 1-D model of Brooks and Glasser (1986) using bifurcation analysis. In all cases, the model indicated that no ignited solutions existed for sufficiently high levels of convection due to heat removal from the stockpile. Brooks et al. (1988c) later modified the model to improve the conditions specified at the entrance to the "chimney."

In a follow-on study, Brooks et al. (1988a) applied a 2-D model to test the assumptions employed in their previous 1-D models. The pile was configured as a frustum with an impermeable, isothermal base and "free" outer surfaces with zero tangential velocity and specified flows normal to the surfaces. These free surfaces allow for prescribed inflow and outflow conditions; however, they do not realistically account for communication between the stockpile and the surrounding environment.

Recently, Bradshaw et al. (1991) studied the effect of natural convection on ignition in a laterally-unbounded coal pile. Both the base and top of the coal layer were held at ambient temperature, and a zero-order reaction was specified within the pile. All flow was assumed to enter and leave through the upper surface of the bed. The critical value of the Frank-Kamenetskii number identifying ignition was calculated as a function of the Rayleigh number, and stable 3-D flow planforms for the model were predicted.

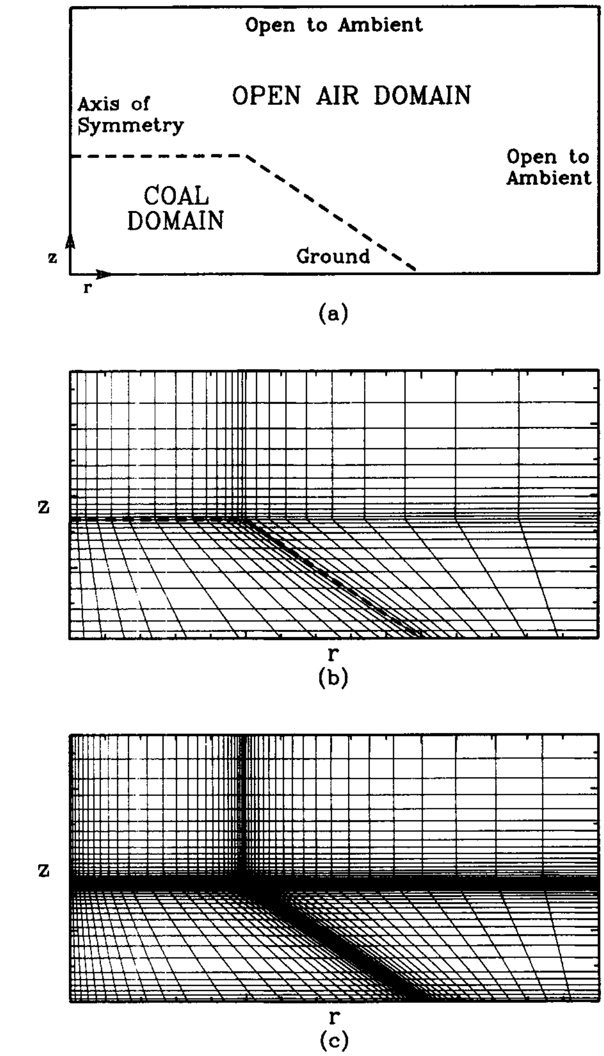

Figure 1. Model with two axisymmetric domains representing the frustum-shaped, porous coal stockpile and homogeneous surrounding air.

(a) Model with two domains and relevant boundaries; (b) mesh M1 with 600 elements and 10,592 total unknowns and used for all calculations except those for $Ra = 2.7 \times 10^{10}$; (c) mesh M2 with 2,064 elements and 35,543 total unknowns and used for the $Ra = 2.7 \times 10^{10}$ calculations.

In all of the above analyses, the models considered fully enclosed porous regions or allowed only for limited communication with the surroundings through specified flows. In reality, there is an important interaction between the reacting porous medium and the atmosphere around the stockpile. Cool air containing oxygen enters the stockpile through the porous boundary of the stockpile, mainly along the sides, and hot combustion gases exit, primarily through the top. The demarcation of net inflow and outflow is not known *a priori*, rather it is determined by the interaction of combustion and flow within the stockpile with the surrounding atmosphere. In addition, a portion of the convective flows simply passes over the coal pile rather than penetrating into it.

Our model assumptions are less restrictive than those employed previously, since flows both within the porous coal pile and in the air surrounding the pile are described, as will be discussed subsequently. By employing a more rigorous approach to describe flows, we hope to provide more realistic predictions for spontaneous ignition and to better understand the underlying physical behavior of the system.

Governing Equations

We employ a novel two-domain model that solves simultaneously for flows in an open porous medium embedded within a homogeneous domain, as shown in Figure 1a. We have adopted the frustum-shaped coal pile geometry of Brooks et al. (1988a) for our study; however, any arbitrary shape could be used to represent the coal pile. Reaction and transport are considered to occur within the coal domain, while transport alone is considered in the surrounding air. The details of this formulation are presented below.

Porous coal pile

The coal pile is modeled as an isotropic, homogeneous porous medium. Heat is transported both by conduction and convection, and is generated by the homogeneous reaction of coal with oxygen. Oxygen is also transported through the pile via diffusion and convection, and is consumed by reaction with the coal. Steady-state, differential heat and species balances lead to the following:

$$\rho C_p(\tilde{v}\cdot\nabla\tilde{T}) = k_c\nabla^2\tilde{T} + k_0(-\Delta H)\frac{\rho}{M_w}\tilde{X}e^{-E/R_g\tilde{T}}, \qquad (1)$$

$$\rho(\tilde{v}\cdot\nabla\tilde{X}) = \mathfrak{D}_c\nabla\cdot(\rho\nabla\tilde{X}) - k_0\rho\tilde{X}e^{-E/R_g\tilde{T}}. \qquad (2)$$

The tilde over several variables indicates dimensional quantities; $\tilde{v}$ is the superficial velocity of fluid within the coal pile, $\tilde{T}$ is the temperature of the medium, and $\tilde{X}$ represents the mole fraction of oxygen. All physical properties are assumed constant except for the fluid density, ρ.

In reality, the kinetics of the coal oxidation reaction are quite complicated, and the combustion of the fully ignited pile will be further complicated by the production ash, the volume shrinkage of the coal particles, and the consumption of carbon (Rajaiah et al., 1988). However, we concentrate here primarily on ignition phenomena and have implemented the simplified kinetic form put forth by Brooks et al. (1988b). The oxidation of the coal is approximated as a pseudo-homogeneous first-order reaction with respect to oxygen concentration (the carbon concentration in the pile is not explicitly considered) with a preexponential factor, k_0, which depends in part on the packing of the pile. Also, we ignore heat effects due to moisture in the stockpile; these effects may be important for the quantitative description of the system (Chen, 1992), but are not likely to fundamentally change the results of our analysis.

We employ Darcy's law to describe the fluid flow in the porous coal domain:

$$\nabla\tilde{P} = -\frac{\mu}{\kappa}\tilde{v} - (\rho-\rho_0)ge_z, \qquad (3)$$

where $\tilde{P}$ is the dimensionless dynamic pressure, which includes the hydrostatic component, $\rho_0 gz$, μ is the viscosity of air, κ is the permeability of the porous medium, which is a function of particle size and packing, ρ_0 is the density of air at ambient conditions, g is the gravitational constant, and $\mathbf{e}_z$ is a unit vector oriented upward in the z-coordinate direction. The continuity equation,

$$\nabla \cdot (\rho \tilde{v}) = 0, \tag{4}$$

insures conservation of mass.

We consider the flow to be incompressible; however, the density of the gas is allowed to vary with temperature using the ideal gas law:

$$\frac{\rho}{\rho_0} = \frac{1}{1+T}, \tag{5}$$

where the dimensionless temperature T is defined with respect to the ambient temperature $\tilde{T}_0$ as, $T = (\tilde{T} - \tilde{T}_0)/\tilde{T}_0$. This approach has been referred to as the generalized anelastic approximation by Lee et al. (1981).

In dimensionless form, the governing equations in the coal pile region are:

$$\frac{1}{1+T}(v \cdot \nabla T) = \frac{1}{Pr_c}\nabla^2 T + \frac{\beta Da}{1+T} X e^{\gamma[T/(1+T)]}, \tag{6}$$

$$\frac{1}{1+T}(v \cdot \nabla X) = \frac{1}{Sc_c}\nabla \cdot \left(\frac{1}{1+T}\nabla X\right) - \frac{Da}{1+T} X e^{\gamma[T/(1+T)]}, \tag{7}$$

$$\nabla P = -\frac{1}{\lambda} v + \left(\frac{T}{1+T}\right)\frac{Ra}{Pr_c \beta}\mathbf{e}_z, \tag{8}$$

$$\nabla \cdot \left(\frac{v}{1+T}\right) = 0. \tag{9}$$

The above equations are scaled with a reference velocity of $\mu/\rho_0 L$, a reference oxygen mole fraction X_0, and the ambient temperature $\tilde{T}_0$. Seven dimensionless groups arise using these scalings—the Prandtl number in the coal domain, Pr_c; the Prater number or dimensionless adiabatic temperature rise, β; the Damkohler number, Da; the Arrhenius number, γ; the Schmidt number in the coal domain, Sc_c; the dimensionless permeability, λ; and the Rayleigh number defined with respect to the adiabatic temperature rise, Ra. The definitions of these groups are:

$Pr_c = \mu C_p / k_c$, $\quad \beta = X_0(-\Delta H)/M_w \tilde{T}_0 C_p$,

$Da = k_0 \rho_0 L^2 e^{-\gamma}/\mu$, $\quad \gamma = E/R_g \tilde{T}_0$,

$Sc_c = \mu/\rho_0 \mathfrak{D}_c$, $\quad \lambda = \kappa/L^2$,

$Ra = \rho_0^2 C_p L^3 \beta_e \tilde{T}_0 g \beta_e / \mu k_c$.

Homogeneous surrounding air

Differential balances for steady-state heat and mass transfer in the air surrounding the coal stockpile do not include reaction terms:

$$\rho C_p(\tilde{v} \cdot \nabla \tilde{T}) = k_a \nabla^2 \tilde{T}, \tag{10}$$

$$\rho(\tilde{v} \cdot \nabla \tilde{X}) = \mathfrak{D}_a \nabla \cdot (\rho \nabla \tilde{X}), \tag{11}$$

where the subscript a refers to the air domain. The steady-state Navier-Stokes equation describes the flow of air in this region:

$$\rho(\tilde{v} \cdot \nabla \tilde{v}) = \nabla \cdot \tilde{\mathbf{T}} - (\rho - \rho_0) g \mathbf{e}_z, \tag{12}$$

with the total stress tensor is defined as:

$$\tilde{\mathbf{T}} = -\left[\tilde{P} + \frac{2\mu}{3}(\nabla \cdot v)\right]\mathbf{I} + \mu(\nabla \tilde{v} + \nabla \tilde{v}^T), \tag{13}$$

where $\mathbf{I}$ is the isotropic tensor or idemfactor. As in the coal pile, the continuity equation ensures mass conservation:

$$\nabla \cdot (\rho \tilde{v}) = 0 \tag{14}$$

We employ the density equation of state, Eq. 5, and nondimensionalize these equations in the same manner as their porous domain counterparts to yield:

$$\frac{1}{1+T}(v \cdot \nabla) T = \frac{1}{Pr_a}\nabla^2 T, \tag{15}$$

$$\frac{1}{1+T}(v \cdot \nabla) X = \frac{1}{Sc_a}\nabla \cdot \left(\frac{1}{1+T}\nabla X\right), \tag{16}$$

$$\frac{1}{1+T}(v \cdot \nabla) v = \nabla \cdot \mathbf{T} + \left(\frac{T}{1+T}\right)\frac{Ra}{Pr_c \beta}\mathbf{e}_z, \tag{17}$$

$$\nabla \cdot \left(\frac{v}{1+T}\right) = 0, \tag{18}$$

where the dimensionless stress tensor is:

$$\mathbf{T} = -\left[P + \frac{2}{3}(\nabla \cdot v)\right]\mathbf{I} + (\nabla v + \nabla v^T). \tag{19}$$

Two new dimensionless groups arise in the formulation for the surrounding air, the Prandtl number and the Schmidt number:

$$Pr_a = \frac{\mu C_p}{k_a} \text{ and } Sc_a = \frac{\mu}{\rho \mathfrak{D}_a},$$

respectively. These groups vary from those defined in the porous domain due to differing physical properties of the two regions. The thermal conductivity of the coal domain is a composite value for air and coal but is dominated by the value for coal. Similarly, the value of the oxygen diffusivity in the coal pile is significantly less than the value in air; we assume that $\mathfrak{D}_c = \mathfrak{D}_a/\tau$, where τ is a tortuosity factor which depends on the porosity and configuration of the porous medium representing the coal stockpile (Cussler, 1984; Epstein, 1989).

Boundary conditions

The imposition of boundary conditions for the field equations presented in the prior two sections must accommodate the multiple goals of physical correctness, mathematical well-posedness, and model expedience. These matters are complicated by the different field equations employed in the two domains, requiring a careful matching at the surface of the coal stockpile. In addition, appropriate far-field boundary conditions must be supplied for the surrounding air region. Below, we briefly put forth our approach; more detailed information is provided by Salinger et al. (1993b).

Conditions for the temperature and concentration across the coal stockpile surface are obtained from straightforward arguments of the continuity of fields and fluxes:

$$T|_a = T|_c, \tag{20}$$

$$\frac{1}{Pr_a}(\boldsymbol{n}\cdot\nabla T)|_a = \frac{1}{Pr_c}(\boldsymbol{n}\cdot\nabla T)|_c, \tag{21}$$

$$X|_a = X|_c, \tag{22}$$

$$\frac{1}{Sc_a}(\boldsymbol{n}\cdot\nabla X)|_a = \frac{1}{Sc_c}(\boldsymbol{n}\cdot\nabla X)|_c, \tag{23}$$

where the subscripts a and c refer to quantities on the air and coal sides of the air/stockpile interface, respectively, and $\boldsymbol{n}$ is a unit vector normal to the surface.

The boundary conditions for the fluid velocity between the two domains are complicated by the mathematical form of Darcy's law, Eq. 3, within the coal pile and the Navier-Stokes relation, Eq. 12, outside of the coal pile. While two conditions are needed for the Navier-Stokes equations, only one condition can be specified for Darcy's law. We require that the normal components of velocity and stress balance across the coal stockpile surface:

$$\boldsymbol{n}\cdot\boldsymbol{v}|_a = \boldsymbol{n}\cdot\boldsymbol{v}|_c, \tag{24}$$

$$\boldsymbol{n}\cdot\boldsymbol{n}\cdot\boldsymbol{T}|_a = -P|_c. \tag{25}$$

A generalized form of the Beavers-Joseph slip condition (Beavers and Joseph, 1967) is used for the final condition:

$$\boldsymbol{n}\cdot\boldsymbol{t}\cdot\boldsymbol{T}|_a = \frac{\alpha}{\sqrt{\lambda}}(\boldsymbol{t}\cdot\boldsymbol{v}|_a - \boldsymbol{t}\cdot\boldsymbol{v}|_c), \tag{26}$$

where $\boldsymbol{t}$ is a unit vector tangent to the surface and α is an empirical slip coefficient. The above vectorial form of the Beavers-Joseph condition was previously employed by Jones (1973) and relates the tangential stress of the open fluid on the interface to a slip, or discontinuity, in the tangential velocity. This equation has gained acceptance as the method of choice for linking a Darcy flow region to a Navier-Stokes region (Prasad, 1991; Salinger et al., 1993b).

The base of the computational domain is taken to be the ground, therefore we impose no normal flow and no flux of oxygen through this surface:

$$\left.\begin{aligned} \boldsymbol{e}_z\cdot\boldsymbol{v}=0,\\ \boldsymbol{e}_z\cdot\nabla X=0, \end{aligned}\right\} \; 0\le r\le R,\; z=0. \tag{27}$$

In the homogeneous air region, we also require no-slip for the tangential velocity:

$$\boldsymbol{e}_r\cdot\boldsymbol{v}=0,\; R_c\le r\le R,\; z=0. \tag{28}$$

We consider two different conditions for the temperature field: either the ground is taken to be the ambient temperature,

$$T=0,\; 0\le r\le R,\; z=0, \tag{29}$$

or the ground is considered to be perfectly insulating,

$$\boldsymbol{e}_z\cdot\nabla T=0,\; 0\le r\le R,\; z=0. \tag{30}$$

Far-field boundary conditions are supplied for the side and top of the computational domains. Since the boundaries are artificial and set merely for computational convenience, we desire that they not strongly influence the behavior of the model system. We impose stress-free conditions at these boundaries for the flow equations:

$$\left.\begin{aligned} \boldsymbol{e}_r\cdot\boldsymbol{e}_r\cdot\boldsymbol{T}=0,\\ \boldsymbol{e}_z\cdot\boldsymbol{e}_r\cdot\boldsymbol{T}=0, \end{aligned}\right\} \; r=R,\; 0\le z\le Z, \tag{31}$$

and

$$\left.\begin{aligned} \boldsymbol{e}_z\cdot\boldsymbol{e}_z\cdot\boldsymbol{T}=0,\\ \boldsymbol{e}_r\cdot\boldsymbol{e}_z\cdot\boldsymbol{T}=0, \end{aligned}\right\} \; 0\le r\le R,\; z=Z. \tag{32}$$

We set the temperature and oxygen concentration at ambient conditions along the side of the computational domain:

$$\left.\begin{aligned} T=0,\\ X=1, \end{aligned}\right\} \; r=R,\; 0\le z\le Z. \tag{33}$$

The top of the computational domain is placed high enough so that the temperature and oxygen concentration gradients normal to this boundary can be assumed to be zero:

$$\left.\begin{aligned} \boldsymbol{e}_z\cdot\nabla T=0,\\ \boldsymbol{e}_z\cdot\nabla X=0, \end{aligned}\right\} \; 0\le r\le R,\; z=Z. \tag{34}$$

Care is taken to ensure that these far-field conditions are placed far enough away as not to significantly effect the solution near the pile.

Finally, axisymmetry is enforced along the origin of the radial coordinate system:

$$\left.\begin{aligned} \boldsymbol{e}_r\cdot\boldsymbol{v}=0,\\ \boldsymbol{e}_r\cdot\nabla T=0,\\ \boldsymbol{e}_r\cdot\nabla X=0, \end{aligned}\right\} \; r=0,\; 0\le z\le Z,$$

$$\boldsymbol{e}_r\cdot\boldsymbol{e}_z\cdot\boldsymbol{T}=0,\; r=0,\; Z_c\le z\le Z. \tag{35}$$

Because of the lower order of Darcy's law, one fewer boundary condition is needed where the coal pile meets the boundary than where the open air meets the boundary; this is reflected in the last condition listed in Eq. 35.

Numerical Methods

There are several interesting features of the numerical approach employed to solve the equations and boundary conditions discussed earlier. We briefly outline our approach below; a more comprehensive discussion and further results which focus on implementation issues are presented by Salinger et al. (1993b).

A finite-element mesh is constructed over both of the model domains with elemental boundaries falling on the surface of the coal stockpile; the meshes used here are shown in Figures 1b and 1c. In the porous coal region, the temperature, concentration, and pressure fields are approximated by biquadratic basis functions, ϕ^i (Dhatt and Touzot, 1984), as:

$$\begin{bmatrix} T(r,z) \\ X(r,z) \\ P(r,z) \end{bmatrix} = \sum_{i=1}^{N_c} \begin{bmatrix} T^i \\ X^i \\ P^i \end{bmatrix} \phi^i(r,z), \tag{36}$$

where the coefficients T^i, X^i, and P^i are mathematical unknowns for these expansions in the porous region, and N_c is the total number of nodes in this region. Rather than directly discretizing the velocity field in the porous region, we calculate it instead from the pressure field solution by rewriting Eq. 8 explicitly for velocity:

$$v = -\lambda \nabla P + \left(\frac{T}{1+T}\right) \frac{\lambda Ra}{Pr_c \beta} e_z. \tag{37}$$

This expression is substituted into the remaining Eqs. 6, 7, and 9 to yield three equations which depend only on temperature, oxygen mole fraction, and dynamic pressure. This approach is particularly advantageous, since it allows the normal force boundary conditions across the interface, Eq. 25, to be implemented easily using the Galerkin weak form of the equations (Salinger et al., 1993b). Additional benefits from this formulation include a reduction in the mathematical degrees of freedom for the problem and avoidance of potential numerical scaling difficulties between the velocity field in the air and the superficial velocity in the coal pile.

In the open-air region, the four variables T, X, v_r, and v_z are approximated using expansions of biquadratic basis functions, while piecewise linear, discontinuous basis functions, Γ^i, approximate the pressure:

$$\begin{bmatrix} v_r(r,z) \\ v_z(r,z) \\ T(r,z) \\ C(r,z) \end{bmatrix} = \sum_{i=1}^{N_a} \begin{bmatrix} v_r^i e_r \\ v_z^i e_z \\ T^i \\ C^i \end{bmatrix} \phi^i(r,z), \tag{38}$$

$$P(r,z) = \sum_{i=1}^{N_{a,p}} P^i \Gamma^i(r,z), \tag{39}$$

where v_r^i and v_z^i are the velocity unknowns, N_a is the number of nodes, and $N_{a,p}$ are the number of pressure unknowns, all defined for the air region. This mixed-order formulation has been demonstrated to be particularly efficient in the Galerkin finite-element method for representing buoyant flows in prior studies (Engelman et al., 1982; Winters, 1988; Salinger et al., 1993c).

Galerkin's method is applied to the field equations, which are integrated over the problem domains and weighted by multiplication of the appropriate basis function. The equations with second-order derivatives are then reduced to the weak form via integration by parts (Dhatt and Touzot, 1984). The finite-element expansion coefficients associated with Dirichelet conditions are set directly to the value specified by the boundary condition, while all other boundary conditions are imposed through the weak form.

The integral form of the Galerkin weighted residual equations are evaluated using nine-point Gaussian quadrature, and the resulting set of nonlinear algebraic equations are solved using the Newton-Raphson method (Dahquist and Björck, 1974). Pseudo-arc length continuation (Keller, 1977) is implemented to track the solutions as a function of a system parameter, which for this work is the Damköhler number. The augmented Jacobian matrix has an "arrow" structure; it is banded except for the final row and column which are full due to components associated with the continuation routine. A direct solver written specifically for this type of matrix structure is used to solve the linear system (Thomas and Brown, 1986).

Two finite-element meshes were employed in this study. For this mesh M1, shown in Figure 1b, a single Newton-Raphson iteration required approximately 2 CPU minutes on the Cray X-MP at the Minnesota Supercomputer Center. A complete one-parameter bifurcation diagram required 5–10 CPU hours. Mesh M1 was determined to be of sufficient accuracy for all simulations except those carried out at the highest value of Rayleigh number (Salinger, 1993a). For the calculations with $Ra = 2.7 \times 10^{10}$, a finer mesh was required to resolve the steep boundary layers near the surface of the coal pile. This mesh, shown as mesh M2 in Figure 1c, required 300 CPU seconds per Newton-Raphson iteration on the Cray C-90 at the Minnesota Supercomputer Center.

The positions of the open boundaries in the homogeneous air domain are chosen to minimize the size of the mesh (and thus computational costs) yet still be far enough away so that the solution near the coal stockpile was not significantly affected by their presence. Figure 2 shows the streamfunction for a solution with significant reaction and convection plotted along radial and vertical slices through the model domain for various computational domain widths R and heights Z. We have chosen $R = 1.5$ and $Z = 0.75$ for our calculations, which are large enough to result in converged solutions near the coal pile.

Results

Axisymmetric solutions are computed to the steady-state governing equations for a coal stockpile shaped as a frustum (after the work of Brooks et al., 1988a). We consider the particular shape in Figure 1; the base of the coal pile has a dimensionless radius $R_c = 1$, the dimensionless height of the pile is set at $Z_c = 1/3$, and the outer corner is at the point $(r, z) = (1/2, 1/3)$. The values of the physical properties, parameters, and dimensionless groups employed for our study are listed in Tables 2 and 3 unless otherwise noted. The slip coefficient of the Beavers-Joseph boundary condition, Eq. 26, is taken to be unity for all calculations presented here; computations by Salinger et al. (1993b) showed that model results are relatively insensitive to the value of this parameter.

We have primarily considered the behavior of the model

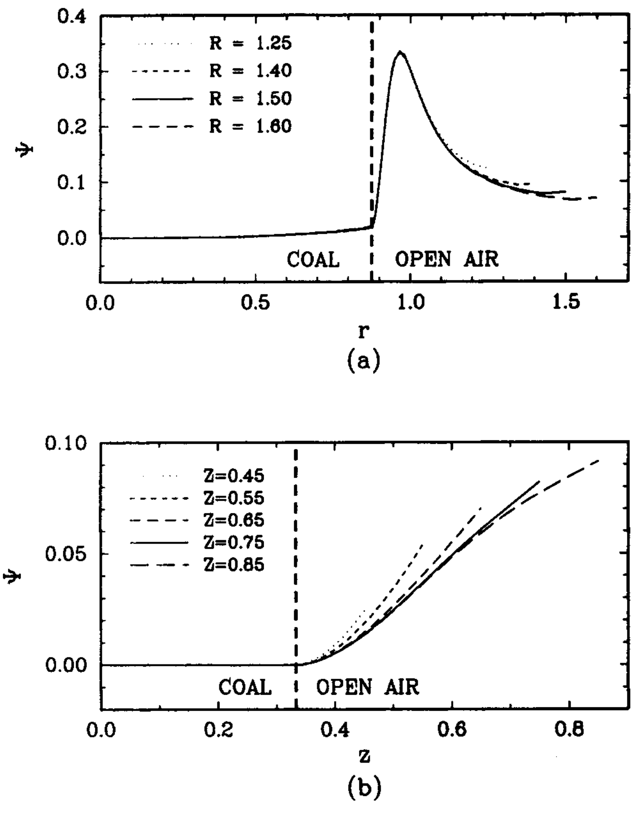

Figure 2. Calculations for an ignited solution (T_{max} = 6.9) of the adiabatic-ground model at $Da = 1.5 \times 10^{-2}$ and $Ra = 6 \times 10^{6}$ for the total size of the computational domain.

(a) Streamfunction at an axial position of $z = 0.1$ as a function of radial distance r for various widths of the computational domain, R; (b) streamfunction at a radial position of $r = 0.167$ as a function of axial distance z for various heights of the computational domain, Z.

with respect to the variation of the dimensionless Damköhler (Da) and Rayleigh (Ra) numbers. The Damköhler number has been varied as the continuation parameter in our bifurcation studies, because coal has a wide variation of reactivities, depending in part on the source and moisture content. The Rayleigh number, which is a strong function of the size of the coal pile, is also varied in the two-parameter studies. It should be noted, however, that varying the length scale in the real system will affect the values of both the Damköhler number and the Rayleigh number. In addition to their physical significance, Da and Ra have traditionally been employed as continuation parameters in the study of chemical reaction and natural convection systems, respectively.

Steady-state solutions of the model

The effects of reactivity and flow on the ignition of the stockpile are explored through the series of bifurcation diagrams in Figure 3, where a stockpile resting on isothermal ground is considered. It shows the maximum dimensionless temperatures of the coal pile, predicted by solutions to the steady-state model developed previously, as functions of the Damköhler number. Five different Rayleigh numbers are considered to examine the behavior of the system with respect to natural convection.

Each curve is S-shaped with a region of three steady-state solutions, thus the model exhibits the classical ignition-extinction behavior of combustion systems. The bottom solution branch corresponds to a low-temperature extinguished state, while the upper branch represents the ignited state. The middle branch represents a set of unstable steady-state solutions, and this branch is connected to the extinguished and ignited branches through turning points, referred to as the ignition and extinction points, respectively. Since we are primarily interested in ignition phenomena in this system, the full S-shaped curves were not calculated for the two highest Rayleigh numbers to conserve computational resources.

Table 2. Values of Physical Constants Used in Calculations

Symbol	Definition	Value	Comments
C_p	Heat capacity of air	1,000 J/kg·K	From Schmal et al. (1985)
$\mathfrak{D}_a$	Diffusivity of oxygen in air	2×10^{-5} m²/s	From Schmal et al. (1985)
$\mathfrak{D}_c$	Diffusivity of oxygen in coal stockpile	4×10^{-6} m²/s	After Nordon & Bainbridge (1979); Cussler (1984); Epstein (1989); $\mathfrak{D}_c = \mathfrak{D}_a/\tau$
D_p	Average coal particle diameter	0.01 m	From Brooks et al. (1988b)
E	Activation energy of coal reaction	58,200 kJ/kmol	From Brooks et al. (1986)
g	Gravitational constant	9.8 m/s²	—
ΔH	Heat of reaction of coal reaction	-3×10^{8} J/kmol	From Brooks et al. (1986)
k_a	Thermal conductivity of air	0.025 W/m·K	From Cussler (1984)
k_c	Effective thermal conductivity of coal stockpile	0.2 W/m·K	From Brooks et al. (1986)
k_0	Pre-exponential rate constant of coal reaction	3,600 s⁻¹	From Brooks et al. (1986); $k_0 = 60(1-\epsilon)/D_p$
L	Characteristic length	1 m	From Brooks et al. (1988b); $L = \tilde{R}_c$
M_w	Molecular weight of air	29.0 kg/kmol	—
$\tilde{R}_c$	Radius of bottom of coal stockpile	1 m	From Brooks et al. (1988b); $\tilde{R}_c = L$
T_0	Ambient temperature	300 K	From Brooks et al. (1986)
X_0	Ambient mole fraction of oxygen	0.21	—
α	Slip coefficient	1	After Beavers et al. (1967); also Salinger et al. (1993b)
β_e	Thermal expansion coefficient of air	1/300 K⁻¹	From ideal gas law; $\beta_e = 1/T_0$
ϵ	Porosity of the coal stockpile	0.4	After Nordon & Bainbridge (1979); Brooks et al. (1988b)
ρ_0	Density of air at ambient conditions	1.18 kg/m³	From Brooks et al. (1986)
τ	Tortuosity of the coal stockpile	5	Estimated from Nordon & Bainbridge (1979); Cussler (1984); Epstein (1989)
κ	Permeability of coal stockpile	1.2×10^{-7} m²	From Ergun (1952); $\kappa = \epsilon^3 D_p^2/150(1-\epsilon)^2$
μ	Viscosity of air	1.8×10^{-5} kg/m·s	From Brooks et al. (1988b)

Table 3. Values of Dimensionless Groups Used in Calculations (Computed from Property Values in Table 2)

Symbol	Dimensionless Group	Definition	Value
Da	Damköhler number	$k_0\rho_0 L^2 e^{-\gamma}/\mu$	0.017*
Pr_a	Prandtl number for air in surrounding atmosphere	$\mu C_p/k_a$	0.72
Pr_c	Prandtl number for air in coal stockpile	$\mu C_p/k_c$	0.09
Ra	Rayleigh number	$\rho_0^2 C_p L^3 \beta_e T_0 g \beta_e/\mu k_c$	2.7×10^{10}*
Sc_a	Schmidt number for air in surrounding atmosphere	$\mu/\rho_0\mathfrak{D}_a$	0.76
Sc_c	Schmidt number for air in coal stockpile	$\mu/\rho_0\mathfrak{D}_c$	3.8
β	Prater number (adiabatic temperature rise)	$X_0(-\Delta H)/M_w T_0 C_p$	7.23
γ	Arrhenius number	$E/R_g T_0$	23.3
λ	Dimensionless permeability	κ/L^2	1.2×10^{-7}*

*Varied in model calculations.

The $Ra=0$ curve represents the case of no convection and shows no multiplicity region and a relatively cold ignited solution. For $Ra>0$, all curves show a region of solution multiplicity. The critical Damköhler number at which ignition occurs first decreases with increasing Rayleigh number and then increases for $Ra\geq6\times10^6$. In addition, as the Rayleigh number is increased the temperature of the ignited solution increases dramatically.

The physics of the ignition-extinction cycle for this system is understood by examining the model solutions at various points along the bifurcation diagram. Three solutions for $Ra=6\times10^6$ are shown in Figures 4, 5, and 6. These figures show contours of streamfunction, dimensionless temperature, and scaled oxygen mole fraction over the coal pile and surrounding air. The four dotted contours on the streamfunction plots as 2, 3, 4, and 5 orders of magnitude below the maximum value attained in the simulation; these streamlines help visualize the faint flows through the coal stockpile.

The solution at the ignition point, $Da=1.1$, is shown in Figure 4. This solution represents the state of maximum reaction rate where heat can still be removed fast enough to prevent ignition and is of most practical importance because it marks the boundary between safe and unsafe conditions for storage. As a turning point on the bifurcation diagram (Figure 3), it also represents the juncture at which steady-state solutions on the extinguished branch lose stability. The streamlines of flow reveal that very little air flows through the coal stockpile

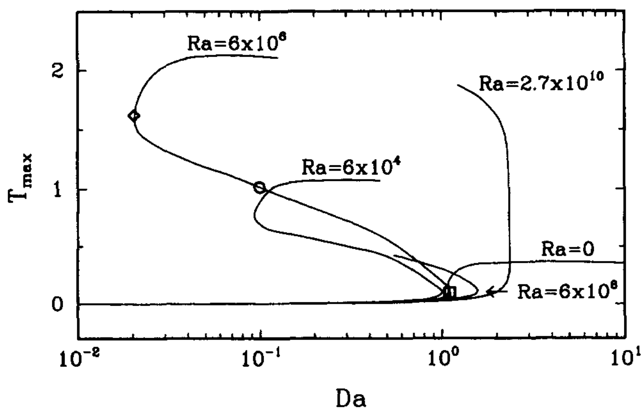

Figure 3. Bifurcation diagrams showing steady-state model solutions of coal reactivity (*Da*) for various levels of natural convection (*Ra*).

These results represent behavior of the coal stockpile situated on cold, isothermal ground.

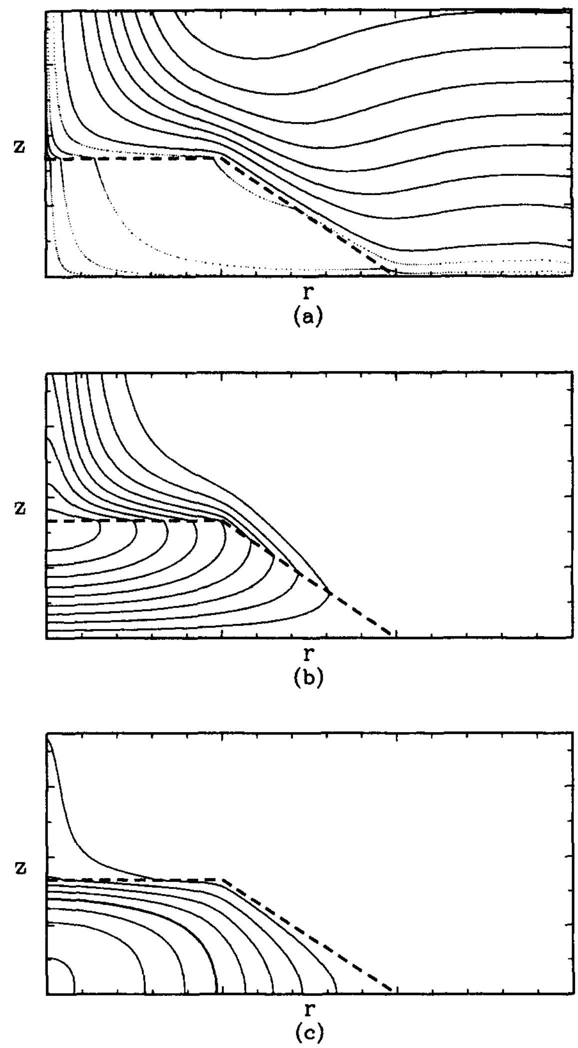

Figure 4. Isothermal-ground solution at the ignition point, $Da=1.1$, $Ra=6\times10^6$.

(a) Streamfunction contours, $\psi_{max}=0.25$, and solid contours spaced at $\Delta\psi=0.03$ (see text for explanation of dotted contours); (b) temperature isotherms, $T_{max}=0.098$, and contour spacing, $\Delta T=0.01$; (c) oxygen mole fraction, $X_{min}=0.60$, and contour spacing, $\Delta X=0.05$.

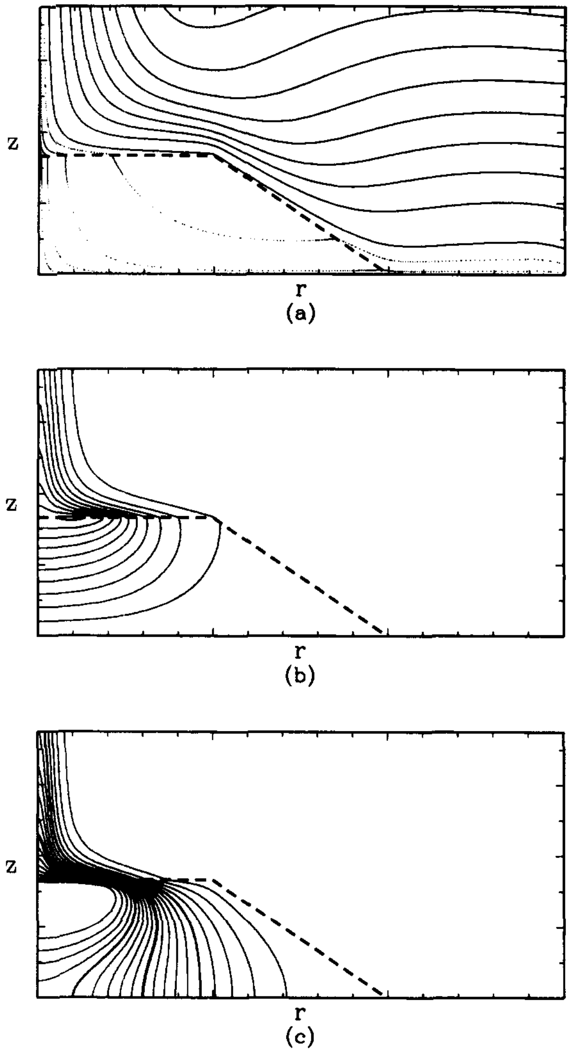

Figure 5. Isothermal-ground solution at an unstable solution, $Da = 0.1$, $Ra = 6 \times 10^6$.

(a) Streamfunction contours, $\psi_{max} = 0.26$, and solid contours spaced at $\Delta\psi = 0.03$ (see text for explanation of dotted contours); (b) temperature isotherms, $T_{max} = 1.02$, and contour spacing, $\Delta T = 0.10$; (c) oxygen mole fraction, $X_{min} = 0.00$, and contour spacing, $\Delta X = 0.05$.

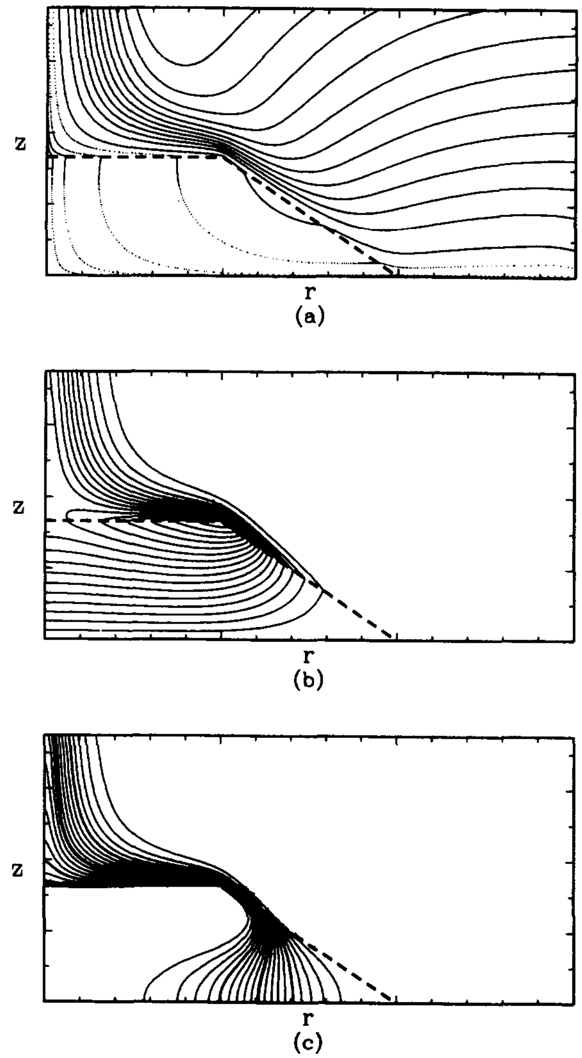

Figure 6. Isothermal-ground solution at the extinction point, $Da = 0.02$, $Ra = 6 \times 10^6$.

(a) Streamfunction contours, $\psi_{max} = 0.50$, and solid contours spaced at $\Delta\psi = 0.04$ (see text for explanation of dotted contours); (b) temperature isotherms, $T_{max} = 1.68$, and contour spacing, $\Delta T = 0.10$; (c) oxygen mole fraction, $X_{min} = 0.60$, and contour spacing, $\Delta X = 0.05$.

directly from the surrounding air. In fact, most of the flow detours around the stockpile. The hot spot is located at the top center of the pile, and there is significant conduction of heat to the cold isothermal ground. The deepest point inside the coal stockpile, $r = 0$ and $z = 0$, is the location most depleted of oxygen. Within the pile, the transport of heat and mass is dominated by conduction and diffusion, while convective effects are apparent in the air surrounding the pile. The discontinuous slopes of the temperature and oxygen contours at the coal/air interface are due to the different physical properties between the coal pile and air, and the significant change in the strength of the fluid flow within and outside of the pile.

A solution from the unstable branch at $Da = 0.1$ is shown in Figure 5. The flow through the pile is much greater than that for the solution at the ignition point, and there are much greater variations in the temperature and oxygen distributions than in the prior case. The hot spot has moved outward from the center of the top surface, and the oxygen is totally depleted in the upper-center section of the pile. Above the pile, heat and mass transfer are dominated by convection caused by a chimney-like flow around the system centerline. This solution represents a mathematical balance between heat generation and removal; however, this steady state is temporally unstable to any disturbance and would likely not be observable in a real system.

The extinction point occurs where the middle solution branch regains stability, Figure 6. This point also marks the last stable solution of the ignited solution branch as the value of the Damköhler number is decreased. The characteristics of this solution quite differ from those shown previously. The flow is uniformly stronger due to the higher buoyant driving forces, and it exhibits boundary layers along the outer surface of the pile. Similar to the prior cases, however, the flow is significantly weakened through the coal pile, and most of the fluid flows around, rather than through, the pile. The hot spot has traveled to the top corner, where the strong convection can

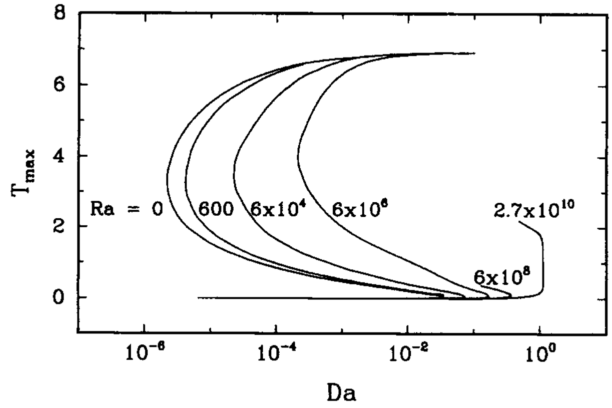

Figure 7. Bifurcation diagrams showing steady-state model solutions of coal reactivity (*Da*) for various levels of natural convection (*Ra*).

These results represent behavior of the coal stockpile with an adiabatic stockpile/ground boundary.

provide the reaction with ample supplies of oxygen. Most of the pile is depleted of oxygen, except for the outer region near the stockpile surface and the lower region where the cold ground quenches the reaction. Boundary layers of temperature and oxygen concentration are apparent along the outer surfaces of the coal pile, while inside the pile, the transport of heat and mass is still dominated by diffusional processes. Convective transport produces a pronounced chimney region above the coal stockpile.

Figure 7 shows a series of bifurcation diagrams calculated for an insulated boundary to the ground. The ignition-extinction behavior of the model with this boundary condition much differs from that predicted for the situation of an isothermal ground. First, note that the maximum temperatures for the ignited solution branches are much larger than the cases shown in Figure 3 and nearly independent of the Rayleigh number. In addition, the ranges of Damköhler numbers over which solution multiplicity occurs are orders of magnitude larger than those for the isothermal ground model, and the critical

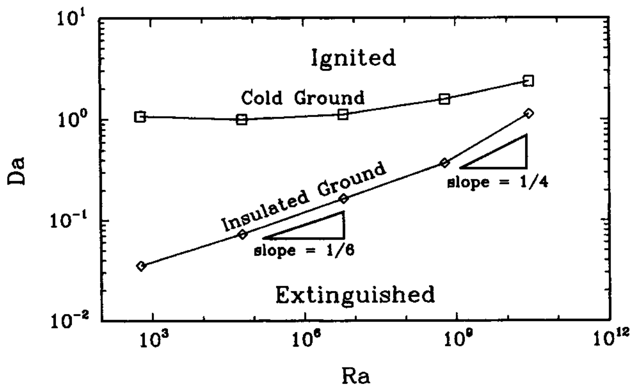

Figure 8. Bifurcation set of extinguished and ignited solutions showing ignition point conditions of Damköhler number, *Da*, and Rayleigh number, *Ra*, for the two different thermal boundary conditions at the ground.

Damköhler numbers for the ignition points have decreased significantly.

These changes are brought about by eliminating heat flow out of the pile to the ground by the insulated ground condition. Conduction of heat from the reacting coal to the cold ground was always significant for the prior model. Since this path for heat transfer is unavailable, the ignited pile reaches a higher temperature for all Damköhler numbers, and much lower reactivities (smaller values of *Da*) are sufficient to ignite the pile from the extinguished state. The broadening of the multiple solution range in *Da* is due to the increased coupling of reaction and flow which arises when conduction to the ground is eliminated.

Another interesting feature of the insulated-ground model is that the location of both turning points increase monotonically with Rayleigh number. The critical Damköhler numbers for the ignition points increase with *Ra* solely due to the increased cooling caused by stronger natural convection at higher Rayleigh numbers. The concomitant increase in the transport of oxygen to the pile via natural convection does not strongly influence the movement of the ignition point with *Ra*. This contention is supported by information obtained from the prior ignition point solution in Figure 4; the oxygen concentration is fairly uniform through the pile (with no depletion regions), therefore mass transfer to the pile must be a minor factor at ignition. The critical value of *Da* at the extinction point also increases with increasing *Ra*. This effect is again explained by the importance of heat transfer from the burning coal; the reaction rate depends more strongly on the temperature of the coal pile—through the Arrhenius term of the kinetic expression—than on the concentration of oxygen. Thus, the higher levels of convection in the surrounding air at higher *Ra* quench the ignited state rather than further promoting reaction by supplying more oxygen to the stockpile.

Ignition conditions

The most useful information provided from modeling the coal stockpile is the prediction of conditions where spontaneous ignition will produce unsafe storage conditions. This information is obtained by tracking the ignition point through parameter space to produce a bifurcation set; Figure 8 shows the dependence of the ignition point on the Rayleigh and Damköhler numbers for both the cold ground and insulated ground models. When the parameter values describing a specific coal pile are above the line, the only stable, steady solution is the ignited state; eventually, such conditions will result in the spontaneous ignition of the pile. Below the line, the extinguished state is stable, and storage of the stockpile is safe.

The ignition point curve displays two regimes for the model which assumes a cold, isothermal ground. For lower Rayleigh numbers, $Ra \leq 10^6$, heat transfer from the slowly reacting pile is accommodated by conduction to the ground, and the ignition point is relatively independent of the level of convective cooling provided by the air flow over the pile. Interestingly, the ignition point decreases slightly with Rayleigh number initially through this regime. Calculations using zero-order reaction kinetics, which are independent of mass transfer, show that ignition occurs at lower Damköhler numbers under these conditions and that the ignition point increases as *Ra* increases (Salinger, 1993a). Consequently, the initial decrease in *Da* for the low Rayleigh number conditions indicates that enhanced oxygen

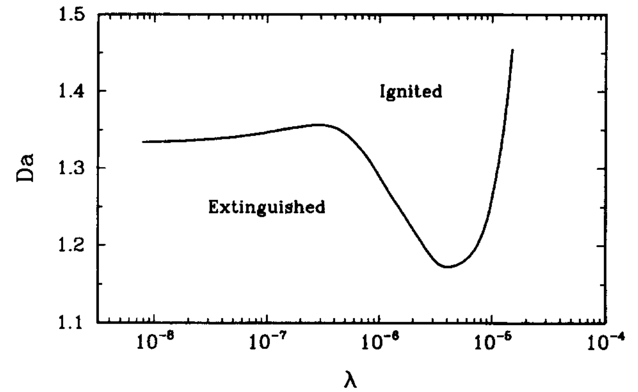

Figure 9. Bifurcation set of extinguished and ignited solutions showing ignition point conditions of Damköhler number, *Da*, and dimensionless permeability, λ, for $Ra = 1.0 \times 10^8$ and the isothermal ground condition.

transport through the pile (via increased natural convection) promotes ignition. This behavior, however, is of little practical interest, since the Rayleigh numbers at which it occurs are far too low to be physically significant in any real system. Convection of heat to the surrounding air becomes important at higher *Ra*, and this additional cooling mechanism delays the onset of ignition to higher Damköhler numbers, as indicated by the slowly rising curve in Figure 8.

The insulated ground model also shows two different behaviors for the ignition point curve. Initially, the ignition point increases monotonically with the Rayleigh number roughly as $Da \sim Ra^{1/6}$. For $Ra \geq 10^9$, there is a stronger dependence of the critical Damköhler number on convective cooling, with the approximate scaling of $Da \sim Ra^{1/4}$. Interestingly, the behavior predicted here is consistent with the cooling of heated bodies or surfaces via natural convection, where the heat-transfer coefficient scales with the Rayleigh number to the one-fourth power (McAdams, 1954). This would be another indication that, for higher Rayleigh numbers, convective flows outside of the coal stockpile, passing over rather than through, predominantly affect the behavior of the system.

The ignition point curves for the two models approach each other as the Rayleigh number is increased. As the Rayleigh number grows larger, heat transfer from the coal pile is dominated by convection from the upper surfaces and the boundary condition along the ground becomes less important. At sufficiently high *Ra*, the two models should exhibit the same asymptotic behavior. Of course, below this limit, ignition points for a real system with a ground which is neither isothermal nor fully insulating would fall somewhere between the curves predicted by the two models.

The dependence of the ignition point on the dimensionless permeability λ and Damköhler number is shown in Figure 9 for the isothermal ground model with $Ra = 10^8$. The critical Damköhler number is a relatively weak function of permeability; however, a minimum in the ignition point is present near $\lambda = 4 \times 10^{-6}$. Since λ was varied independently in these calculations and only appears in Darcy's law, Eq. 3, this effect must be attributed to flow within the coal pile. As the permeability of the stockpile increases, the resistance to flow decreases. The subsequent increase in flow causes increased oxygen transport to the reacting coal and increased heat removal from the stockpile. Since the Schmidt number is much larger than the Prandtl number for the coal region ($Sc_c = 3.8$ and $Pr_c = 0.09$), the convective transport will act to increase mass transport at a faster rate than the associated heat transport. Initially, flow through the pile will fuel the reaction with increased oxygen transport, and the critical reactivity for ignition decreases. As flow through the pile continues to increase with decreasing permeability, two effects will become important: the oxygen concentration will saturate near ambient levels, while the transport of heat will continue to increase. Eventually, the convective cooling acts to quench the reaction, and the critical Damköhler number increases.

Conclusions

A two-domain model has been developed and applied to study the spontaneous ignition of coal stockpiles. For the first time, the flows of the porous coal pile and the homogeneous surrounding air are modeled in a self-consistent manner. The implementation details for describing these flows are put forth in Salinger et al. (1993b). Accounting for flow through the pile and the surrounding air results in predictions for the behavior of this system which are quite different than those obtained by earlier models. Most importantly, the surrounding air preferentially flows around the outside of the pile, and convection plays a relatively minor role inside the pile.

The net effects of flow on the ignited states of the system depend on the assumption made about the conditions at the stockpile/ground interface. For the model which assumes that the ground is isothermal, significant heat loss from the pile to the ground occurs via conduction through the stockpile. This effect results in relatively cold ignited states (compared to the model which assumes an adiabatic ground condition) and reduces the role of convective cooling of the pile. Instead, the convective transport of oxygen supports the ignited pile in this model. A more intense flow (higher *Ra*) better fuels the reaction, which then leads to an increased temperature of the ignited state and a shift of the extinction point to lower values of coal reactivity (smaller *Da*). Different behavior results from the model which assumes the stockpile/ground boundary to be adiabatic. For this assumption, all of the cooling of the stockpile occurs through the upper pile surfaces, so increasing levels of convection (higher Rayleigh numbers) result in a shifting of the extinction point to higher Damköhler numbers—a trend exactly opposite to that predicted by the isothermal ground model.

The ignited-solution branch predicted from our two-domain model exhibits a fundamentally different behavior with respect to intense natural convection than that predicted by previous analyses. In our model, increasing natural convection enhances heat and mass transfer to the coal stockpile by thinning the boundary layer over the exterior stockpile surface. Prior models have assumed that buoyancy drives flows directly through the pile, greatly increasing transport processes through the pile itself. One consequence of this is the prediction of an additional extinction mechanism where large flow rates through the pile quench the ignited solution due to the enhanced cooling caused by the flow (Brooks et al., 1988b). We do not observe this behavior in our model; at larger values of *Ra*, the bulk of the flow is predicted to simply pass over the pile rather than through it, and cooling is not sufficient to quench the ignited state.

Understanding critical ignition point conditions is aided by the bifurcation sets produced by our models. Both models predict that the onset of criticality (with respect to coal reactivity or Damköhler number) is generally delayed with increasing levels of convection; however, the isothermal ground and adiabatic ground models predict very different ignition points at lower Rayleigh numbers. The cooling of the coal stockpile by the ground strongly suppresses spontaneous ignition and, as discussed above, results in lower pile temperatures for the ignited steady state. In addition, this predominant cooling of the stockpile by the isothermal ground leads to a slight decrease of the ignition point with increasing Rayleigh number for $Ra < 10^5$. Only under these conditions does the increased oxygen transfer through the pile via natural convection outweigh the suppression of ignition via exterior convective cooling. At higher Ra, the ignition points for both models approach each other as heat losses from the outer surfaces of the pile begin to dominate ground losses.

The scaling of the ignition point curve for the insulating ground model as $Da \sim Ra^{1/4}$ at high Rayleigh numbers supports our contention that natural convection produces flows primarily over the outer surface of the coal pile and that the dominant factor controlling spontaneous ignition is the heat transfer occurring through the boundary layer adjacent to that outer surface. This differs fundamentally from that of the model put forth by Brooks et al. (1988b) which, for higher Rayleigh numbers, predicts a linear relationship between the critical Damköhler number and Ra. This behavior takes on even greater importance for coal piles larger than the relatively small size considered here. Our model results suggest that a reasonable approximation to the ignition behavior of large stockpiles may be obtained using simple boundary-layer scalings for heat transfer outside the coal pile coupled with diffusion-dominated transport within the stockpile—an approach which is very different from reaction engineering models constructed in the past to describe this system.

Although not nearly important as flow over the pile, convective flow through the pile also affects ignition point conditions. We find that intermediate values of permeability produce the most dangerous conditions for spontaneous ignition. However, this effect is much weaker than effects produced by the flow intensity variations (represented by Ra) discussed above. Earlier models have predicted that piles composed of intermediate-size particles are the most dangerous, while fine or coarse particles are less dangerous (Brooks and Glasser, 1986; Brooks et al., 1988c). However, our results do not directly support this claim: if the particle diameter (D_p) is varied to change the dimensionless permeability, the dimensionless Damköhler number will also change (see the definitions of Da in Table 3 and k_0 in Table 2). If our results are rescaled to plot the ignition point curve in terms of coal reactivity (independent of D_p) and particle diameter, the minimum point on the $Da - \lambda$ ignition curve disappears, and the curve monotonically increases with particle size.

While the model presented here for the analysis of ignition conditions for a coal stockpile is not quantitative, our results indicate behaviors which differ fundamentally from those predicted by previous models. Certainly, more realistic descriptions of reaction chemistry, moisture effects, ground heat transfer, and pile shape and size would be needed for detailed study of this system. In addition, three-dimensional and time-dependent effects, such as local winds, diurnal temperature variations, and inherent dynamic instabilities, may be important to predict real behaviors. Nevertheless, the results shown here clearly demonstrate the need for a self-consistent treatment of flows of the air surrounding the coal pile in modeling this system. Similar approaches for the rigorous representation of transport effects will likely be required for the study of many other systems where flow and reaction are strongly coupled.

Acknowledgment

This work was supported in part by the University of Minnesota Army High Performance Computing Research Center (under the auspices of Army Research Office contract number DAAL03-89-C-0038), the Minnesota Supercomputer Institute, and the donors of The Petroleum Research Fund, administered by the American Chemical Society. AGS would like to acknowledge support in the form of Graduate Fellowships from the National Science Foundation and the Army High Performance Computing Research Center; JJD gratefully acknowledges the National Science Foundation for support through the PYI award program.

Notation

C_p = heat capacity
$\mathfrak{D}$ = diffusion coefficient of oxygen
D_p = average particle diameter
Da = Damköhler number
e = unit coordinate vector
E = activation energy
g = gravitational constant
I = identity tensor
k = thermal conductivity
k_0 = preexponential rate factor
L = characteristic length
M_w = molecular weight of air
n = unit normal vector
P = dynamic pressure
Pr = Prandtl number
q = heat flux
r = radial coordinate
R = radius of computational domain
R_c = radius of coal pile
R_g = universal gas constant
Ra = Rayleigh number
Sc = Schmidt number
t = unit tangent vector
T = dimensionless temperature
T = stress tensor
v = velocity vector
X = oxygen mole fraction
z = axial coordinate
Z = height of computational domain
Z_c = height of coal pile

Greek letters

α = Beavers-Joseph slip coefficient
β = dimensionless adiabatic temperature rise
β_e = coefficient of thermal expansion
γ = Arrhenius number
Γ = linear basis functions
ΔH = heat of reaction
ϵ = porosity of the coal pile
ρ = density of air
θ = azimuthal coordinate
κ = permeability
λ = dimensionless permeability
μ = viscosity of air
τ = tortuosity of coal
Φ = biquadratic basis functions
Ψ = streamfunction

Mathematical symbols

∇ = gradient operator

Subscripts

0 = at ambient conditions
a = in the air domain
c = in the coal domain
max = maximum value
min = minimum value

Superscripts

i = index for degrees of freedom
$\tilde{}$ = unscaled or dimensional quantity

Literature Cited

Aris, R., *The Mathematical Theory of Diffusion and Reaction in a Permeable Catalyst*, Vols. 1 and 2, Oxford University Press, London (1975).

Aris, R., and A. Varma, *The Mathematical Understanding of Chemical Engineering Systems: Selected Papers of Neal R. Amundson*, Pergamon Press, New York (1980).

Balakotaiah, V., and D. Luss, "Multiplicity Features of Reacting Systems," *Chem. Eng. Sci.*, **38**, 1709 (1983).

Balakotaiah, V., and D. Luss, "Global Analysis of the Multiplicity Features of Multiple Reaction Lumped-Parameter Systems," *Chem. Eng. Sci.*, **39**, 865 (1984).

Balakotaiah, V., and P. Pourtalet, "Natural Convection Effects on Thermal Ignition in a Porous Medium: I. Semenov Model," *Proc. Roy. Soc. Lond. A*, **429**, 533 (1990a).

Balakotaiah, V., and P. Pourtalet, "Natural Convection Effects on Thermal Ignition in a Porous Medium: II. Lumped Thermal Model-I," *Proc. Roy. Soc. Lond. A*, **429**, 555 (1990b).

Beavers, G. S., and D. D. Joseph, "Boundary Conditions at a Naturally Permeable Wall," *J. Fluid Mech.*, **30**, 197 (1967).

Bradshaw, S., D. Glasser, and K. Brooks, "Self-Ignition and Convection Patterns in an Infinite Coal Layer," *Chem. Eng. Comm.*, **105**, 255 (1991).

Brooks, K., S. Bradshaw, and D. Glasser, "Spontaneous Combustion of Coal Stockpiles—An Unusual Chemical Reaction Engineering Problem," *Chem. Eng. Sci.*, **43**(8), 2139 (1988a).

Brooks, K., V. Balakotaiah, and D. Luss, "Effect of Natural Convection on Spontaneous Combustion of Coal Stockpiles," *AIChE J.*, **34**(3), 353 (1988b).

Brooks, K., and D. Glasser, "A Simplified Model of Spontaneous Combustion of Coal Stockpiles," *Fuel*, **65**, 1035 (1986).

Brooks, K., N. Svanas, and D. Glasser, "Evaluating the Risk of Spontaneous Combustion in Coal Stockpiles," *Fuel*, **67**, 651 (1988c).

Caltagirone, J. P., "Thermoconvective Instabilities in a Horizontal Porous Layer," *J. Fluid Mech.*, **72**, 269 (1975).

Chen, X. D., "On the Mathematical Modeling of the Transient Process of Spontaneous Heating in a Moist Coal Stockpile," *Comb. and Flame*, **90**, 114 (1992).

Cussler, E. L., *Diffusion: Mass Transfer in Fluid Systems*, Cambridge University Press, Cambridge (1984).

Dahlquist, G., and A. Björck, *Numerical Methods*, translated by N. Anderson, Prentice-Hall, Englewood Cliffs, NJ (1974).

Dhatt, G., and G. Touzot, *The Finite Element Method Displayed*, Wiley, New York (1984).

Engelman, M., R. L. Sani, P. M. Gresho, and M. Bercovier, "Consistent vs. Reduced Integration Penalty Methods for Incompressible Media Using Several Old and New Elements," *Int. J. Num. Meth. Fluids*, **2**(1), 25 (1982).

Epstein, N., "On Tortuosity and the Tortuosity Factor in Flow and Diffusion Through Porous Media," *Chem. Eng. Sci.*, **44**, 777 (1989).

Ergun, S., "Fluid Flow Through Packed Columns," *Chem. Eng. Prog.*, **48**, 89 (1952).

Farr, W. W., J. F. Gabitto, D. Luss, and V. Balakotaiah, "Reaction-Driven Convection in a Porous Medium," *AIChE J.*, **37**, 963 (1991).

Frank-Kamenetskii, D. A., *Diffusion and Heat Transfer in Chemical Kinetics*, 2nd ed., Plenum Press, New York (1969).

Gatica, J. E., H. J. Viljoen, and V. Hlavacek, "Interaction Between Chemical Reaction and Natural Convection in Porous Media," *Chem. Eng. Sci.*, **44**, 1853 (1989).

Hlavacek, V., *Dynamics of Nonlinear Systems*, Gordon and Breach, New York (1986).

Jensen, K. F., "Micro-Reaction Engineering: Applications of Reaction Engineering to Processing of Electronic and Photonic Materials," *Chem. Eng. Sci.*, **42**(5), 923 (1987).

Jensen, K. F., and W. H. Ray, "The Bifurcation Behavior of Tubular Reactors," *Chem. Eng. Sci.*, **37**, 199 (1982).

Jones, D. R., "Convective Effects in Enclosed Exothermically Reacting Gases," *Int. J. Heat Mass Transfer*, **17**, 11 (1974).

Jones, I. P., "Low Reynolds Number Flow Past a Porous Spherical Shell," *Proc. Camb. Phil. Soc.*, **73**, 231 (1973).

Keller, H. B., "Numerical Solution of Bifurcation and Nonlinear Eigenvalue Problems," *Applications of Bifurcation Theory*, P. H. Rabinowitz, ed., Academic Press, New York, 359 (1977).

Kordylewski, W., and Z. Krajewski, "Convection Effects on Thermal Ignition in Porous Media," *Chem. Eng. Sci.*, **39**, 610 (1984).

Lapwood, E. R., "Convection of a Fluid in a Porous Medium," *Proc. Camb. Phil. Soc.*, **44**, 508 (1948).

Lee, R. L., P. M. Gresho, S. T. Chan, and C. D. Upson, "A Three-Dimensional Finite Element Model for Simulating Heavier-Than-Air Gaseous Releases Over Variable Terrain," *Air Pollution Modeling & Its Application*, C. De Wispelaere, ed., 555 (1983); Lawrence Livermore National Laboratory Report UCRL-85520, Livermore, CA (1981).

McAdams, W. H., *Heat Transmission*, 3rd ed., McGraw-Hill, New York (1954).

Merzhanov, A. G., and E. A. Shtessel, "Free Convection and Thermal Explosion in Reactive Systems," *Acta Astronautica*, **18**, 191 (1973).

Nordon, P., "A Model for the Self-Heating Reaction of Coal and Char," *Fuel*, **58**, 456 (1979).

Nordon, P., and N. W. Bainbridge, "Some Properties of Char Affecting the Self-Heating Reaction in Bulk," *Fuel*, **58**, 450 (1979).

Nordon, P., B. C. Young, and N. W. Bainbridge, "The Rate of Oxidation of Char and Coal in Relation to Their Tendency to Self-Heat," *Fuel*, **58**, 443 (1979).

Prasad, V., "Convective Flow Interaction and Heat Transfer Between Fluid and Porous Layers," *Convective Heat and Mass Transfer in Porous Media*, S. Kakac et al., eds., Kluwer Academic Publishers, 563 (1991).

Rajaiah, J., H. Dandekar, J. Puszynski, J. Degreve, and V. Hlavacek, "Study of Gas-Solid, Heterogeneous, Exothermic, Noncatalytic Reactions in a Flow Regime," *Ind. Eng. Chem. Res.*, **27**, 513 (1988).

Salinger, A. G., "The Nonlinear Coupling of Transport and Reaction," PhD Thesis, Dept. of Chemical Engineering and Materials Science, Univ. of Minnesota (1993a).

Salinger, A. G., R. Aris, and J. J. Derby, "Finite Element Formulations for Large-Scale, Coupled Flows in Adjacent Porous and Open Fluid Domains," *Int. J. Num. Meth. Fluids*, in press (1993b).

Salinger, A. G., S. Brandon, R. Aris, and J. J. Derby, "Buoyancy-Driven Flows of a Radiatively Participating Fluid in a Vertical Cylinder Heated from Below," *Proc. R. Soc. Lond. A*, **442**, 313 (1993c).

Schmal, D., J. H. Duyzer, and J. W. van Heuven, "A Model for the Spontaneous Heating of Coal," *Fuel*, **64**, 963 (1985).

Shtessel, E. A., K. V. Pribytkova, and L. A. Zhukova, "Characteristics of Thermal Self-Ignition Under Conditions of Natural Convection," *Fiz. Goren. Vzryva*, **15**, 3 (1978).

Song, X., W. R. Williams, L. D. Schmidt, and R. Aris, "Bifurcation Behavior in Homogeneous-Heterogeneous Combustion: II. Computations for Stagnation-Point Flow," *Comb. and Flame*, **84**, 292 (1991).

Strauss, J. M., "Large Amplitude Convection in a Porous Media," *J. Fluid Mech.*, **64**, 51 (1974).

Thomas, P. D., and R. A. Brown, "LU Decomposition of Banded Matrices With Augmented Dense Constraints," *Int. J. Numer. Methods Eng.*, **24**, 1451 (1986).

Uppal, A., W. H. Ray, and A. B. Poore, "On the Dynamic Behavior of Continuous Stirred Tank Reactors," *Chem. Eng. Sci.*, **29**, 967 (1974).

van Doornum, G. A. W., "The Spontaneous Heating of Coal," *J. Inst. Fuel*, **27**, 482 (1954).

Viljoen, H. J., J. E. Gatica, and V. Hlavacek, "Induction Times for Thermal Explosion and Natural Convection in Porous Media," *Chem. Eng. Sci.*, **43**, 2951 (1988).
Viljoen, H. J., and V. Hlavacek, "Chemically Driven Convection in Porous Medium," *AIChE J.*, **33**, 1344 (1987).
Williamson, R. T., "Coal Handling—An Operations View Point," *Coal Technology '82*, Vol. 2, 117 (1982).
Winters, K. H., "Laminar Natural Convection in a Partially Divided Rectangular Cavity at High Rayleigh Number," *Int. J. Numer. Meth. Fluids*, **8**, 247 (1988).
Young, B. D., D. F. Williams, and A. W. Bryson, "Two-Dimensional Natural Convection and Conduction in a Packed Bed Containing a Hot Spot and its Relevance to the Transport of Air in a Coal Dump," *Int. J. Heat Mass Transfer*, **29**, 331 (1986).
Zeldovich, Y. B., and D. A. Frank-Kamenetskii, "Thermal Theory of Flame Propagation," *Zh. Phys. Chim.*, **12**, 100 (1938).

Manuscript received June 21, 1993, and revision received Aug. 23, 1993.